



Sharp changes in plant diversity and plant-herbivore interactions during the Eocene–Oligocene transition on the southeastern Qinghai-Tibetan Plateau



Weiyudong Deng^{a,b,c}, Tao Su^{a,b,c,*}, Torsten Wappler^d, Jia Liu^{a,b}, Shufeng Li^{a,b}, Jian Huang^{a,b}, He Tang^{a,b,c}, Shook Ling Low^{a,b}, Tengxiang Wang^{a,b,c}, He Xu^e, Xiaoting Xu^{a,b,c}, Ping Liu^a, Zhekun Zhou^{a,b,*}

^a CAS Key Laboratory of Tropical Forest Ecology, Xishuangbanna Tropical Botanical Garden, Chinese Academy of Sciences, Mengla 666303, Yunnan, China

^b Center of Plant Ecology, Core Botanical Gardens, Chinese Academy of Sciences, Mengla 666303, Yunnan, China

^c University of Chinese Academy of Sciences, Beijing 100049, China

^d Hessisches Landesmuseum Darmstadt, Darmstadt 64283, Germany

^e Institute of Geology and Paleontology, Linyi University, Linyi 276000, Shandong, China

ARTICLE INFO

Keywords:

Plant-herbivore interactions
Leaf fossil
Uplift
Eocene
Oligocene
Climate change

ABSTRACT

Herbivore damage patterns on fossil leaves are essential to explore the evolution of plant-herbivore interactions under paleoenvironmental changes and to better understand the evolutionary history of terrestrial ecosystems. The Eocene–Oligocene transition (EOT) is a period of dramatic paleoclimate changes that significantly impacted global ecosystems; however, the influences on plant-herbivore interactions during this period are largely unknown. We identified taxonomic composition of the flora, and investigated well-preserved herbivore damage on fossil leaves from two layers of the Lawula Formation in Markam County, southeastern Qinghai-Tibetan Plateau (QTP), China. Besides, paleoclimate conditions were reconstructed using fossil plant assemblages. The plant assemblage from the latest Eocene layer (MK-3, ~34.6 Ma) was dominated by Fagaceae and Betulaceae, whereas Rosaceae and Salicaceae were the most abundant in the earliest Oligocene layer (MK-1, ~33.4 Ma). In MK-3, 932 out of 2428 fossil leaves were damaged and presented 41 damage types (DTs). The richest functional feeding groups (FFGs) in this layer were hole feeding, margin feeding, and galling. In MK-1, 144 out of 599 leaves were damaged and presented 20 DTs, with the major FFGs being hole feeding, margin feeding, and skeletonization. Generally, MK-3 had a significantly higher damage frequency (DF) and more DTs compared to MK-1. The decline in temperature, accompanied by the mountain uplift during the EOT on the QTP margin, led to changes in plant composition, with a consequent decrease in herbivory quantity and diversity. Our results shed new light on the influence of paleoenvironmental changes in shaping the evolution of biodiversity as well as the ecosystem on the plateau.

1. Introduction

Herbivore damage patterns, caused by feeding, nesting and other behaviors, are the main parameters for tracing the relationships between herbivores and plants (Schoonhoven et al., 2005). Most of these relationships are linked to nutrient consumption and are vital to all terrestrial ecosystems; they account for more than 75% of the worldwide nutrient webs, making them key factors for the stabilization of the biosphere (Price, 2002). Currently, changes in global temperatures pose a significant threat to terrestrial ecosystems. Against this background, and considering the increasing interest in the influences on global

plant-herbivore interactions, there is a growing number of studies focusing not only on present ecosystems (Zvereva and Kozlov, 2006; Massad and Dyer, 2010), but also on these issues in the geological past.

Damage frequency (DF) and damage types (DTs) are two commonly used indices to describe plant-herbivore interactions which can reflect herbivore quantity, consumption, and diversity (Schachat et al., 2018, 2020). Many factors could contribute to the plant-herbivore interactions. Generally, they are shaped by the mixture influence of different factors such as temperature, carbon dioxide, precipitation (Zvereva and Kozlov, 2006; Loughnan and Williams, 2018), and elevational gradients (Adroit et al., 2018; Sohn et al., 2019; Sam et al., 2020). The regional

* Corresponding authors at: CAS Key Laboratory of Tropical Forest Ecology, Xishuangbanna Tropical Botanical Garden, Chinese Academy of Sciences, Mengla 666303, Yunnan, China.

E-mail addresses: sutao@xtbg.org.cn (T. Su), zhouzk@xtbg.ac.cn (Z. Zhou).

<https://doi.org/10.1016/j.gloplacha.2020.103293>

Received 20 April 2020; Received in revised form 31 July 2020; Accepted 7 August 2020

Available online 11 August 2020

0921-8181/ © 2020 Elsevier B.V. All rights reserved.

differences in climatic factors are the major drivers of the global diversification of DF and DTs (Adams et al., 2010, 2011), as they directly influence both plants and herbivores in an ecosystem (Bale et al., 2002; Blois et al., 2013). These climatic factors form the global patterns of herbivore quantity, consumption, and diversity (Tylianakis et al., 2008).

Herbivore-damaged plant fossils extensively reported from fossil floras in Europe and North America, proved to be efficient to trace herbivore richness in response to paleoenvironmental changes in ancient terrestrial ecosystems (Wappler et al., 2009, 2012; Carvalho et al., 2014). Because in most cases only few herbivore fossils could be found together with a fossil leaf assemblage, investigations of insect damage on plant fossils provide opportunities for the understanding of herbivore activities under paleoenvironmental changes in the geological past. For instances, damage patterns were used to trace the influence of paleoclimate changes on herbivores during significant environmental events, such as the Paleocene/early Eocene global warming (Wilf and Labandeira, 1999), the Miocene regional cooling in South Korea (Paik et al., 2012), and the Quaternary climate fluctuations in southwestern China (Su et al., 2015).

The Eocene–Oligocene transition (EOT) is an important time interval in the Cenozoic, when the global climate shifted from the ‘greenhouse’ to the ‘icehouse’ (Zachos et al., 2001; Katz et al., 2008). Evidence from isotope, weathering, sea retreat, and tectonic movement revealed that the Earth had encountered a temperature drop within a short geological time (Allen and Armstrong, 2008; Liu et al., 2009; Basak and Martin, 2013). Under such events, dramatic flora and fauna turnovers occurred in different continents (Meng and McKenna, 1998; Hooker et al., 2004; Sun et al., 2014), but evidence from the Asian flora (Fig. 1A) is still far from sufficient (Dupont-Nivet et al., 2008; Abels et al., 2011). The effects of these paleoenvironmental changes on plant-herbivore interactions in this large region are still poorly understood.

This study provides comprehensive evidence of plant-herbivore interactions during the EOT on the Qinghai-Tibetan Plateau (QTP) by incorporating two leaf assemblages from the Markam Basin in the southeastern margin of the QTP that existed within a short period of the EOT. The objectives of this study are to understand the pattern of plant-herbivore interactions under different plant diversity conditions within the same site, and to demonstrate how the EOT climate change and the QTP marginal uplift influenced contemporaneous plant-herbivore interactions, which could provide important evidence for the evolutionary history of the terrestrial ecosystem on the plateau.

2. Materials and methods

2.1. Geological setting

The Markam Basin (29°45'N; 98°25'E; Fig. 1A) is located on the southeastern margin of the QTP. The bottom section of the basin consists of Cretaceous deposits of calcareous brick-red quartz sandstones, calcareous siltstones, and mudstones interbedded with gypsum. The upper part is the Eocene–Oligocene Lawula Formation composed of conglomerates, pebbly sandstones, mudstones and volcanic rocks (Fig. 1B). The geological background has been described in detail in Su et al. (2019b).

Fossils were collected from the Lawula Formation in Kajun Village, which is about 16 km northwest of the Gatuo Town, Markam County. There are four plant fossil assemblages, namely MK-1 to MK-4, in the Lawula Formation (Fig. 1B); plant fossils are the most abundant in MK-1 and MK-3. The ages of MK-1 (33.4 ± 0.6 Ma) and MK-3 (34.6 ± 0.8 Ma) have been radiometrically dated by $^{40}\text{Ar}/^{39}\text{Ar}$ analysis (Su et al., 2019b). In total, 599 leaf specimens were collected from MK-1, and 2428 fossil leaf specimens were collected from MK-3. For this flora, some species have been previously reported, i.e., *Equisetum oppositum* H. J. Ma, T. Su et S. T. Zhang (Ma et al., 2012), *Elaeagnus tibetensis* T. Su et Z. K. Zhou (Su et al., 2014), *Quercus tibetensis* H. Xu, T.

Su et Z. K. Zhou (Xu et al., 2016), *Alnus cf. ferdinandi-coburgii* C. K. Schneid (Xu et al., 2019), *Tsuga cf. dumosa* (Don) Eichler (Wu et al., 2019), and *Berchamniphyllum junrongii* Z. K. Zhou, T. X. Wang et J. Huang (Zhou et al., 2020).

2.2. Sampling and fossil identification

All leaf fossils in this study were digitalized using a Nikon D700. After this standardized treatment, we created a leaf specimen dataset of the Markam flora. All fossils were deposited in Paleocology Collections, Xishuangbanna Tropical Botanical Garden (XTBG), Chinese Academy of Sciences.

Identification of MK-1 and MK-3 leaf assemblages was partly based on previous studies, combined with referring to contemporary floras of the Northern Hemisphere (Berry, 1916; Manchester, 2001), and modern specimens from herbaria of Kunming Institute of Botany (KUN) and Xishuangbanna Tropical Botanical Garden (HITBC). In this study, except for the taxonomically identified specimens, fossil leaves with similar features such as leaf shape, venation, and leaf margin were assigned to the same morphotype. Plant reproductive organs, including tubers, inflorescences, and cones, were also identified for reconstructing paleoclimate (Table 1).

2.3. Identification of damage types

Examination of plant-herbivore interactions followed the ‘Guide to Insect (and other) Damage Types on Compressed Plant Fossils’ (Labandeira et al., 2007), which assigns damage morphologies of fossil leaves to different types (DTs) with detailed morphological descriptions, and uses functional feeding groups (FFGs) to determine different functional types of DTs. The DTs on the fossil leaves were examined using a Leica S8APO stereoscope and photographed using a Leica DFC295 digital microscope in the laboratory of the Paleocology Research Group (PRG), XTBG. All FFGs and DTs on each leaf were compiled in one dataset.

2.4. Data analyses

Rarefaction models of the EstimateS (v. 9.0) software and the iNEXT (v. 2.0.20) package in R (v. 3.6.2) were used to quantitatively analyze data of samples collected from two different layers (Colwell et al., 2012; Chao et al., 2014). We also applied the rarefaction method developed by Gunkel and Wappler (2015) to eliminate the sampling size bias (constrained in the level of 600 samples).

The paleoclimate reconstructions using leaf assemblages from the Markam Basin are based on Leaf Margin Analysis (LMA) and the Coexistence Approach (CA). The LMA is estimated by a model with single linear regression method, based on 50 modern samples in China (Su et al., 2010). The CA is based on the assumption that fossil taxa had climate requirements similar to those of their nearest living relatives (Mosbrugger and Utescher, 1997). For CA, the spatial distribution of each taxon was retrieved from the GBIF (Global Biodiversity Information Facility, <https://www.gbif.org>), and the climate indices were downloaded from the WorldClim (<http://www.worldclim.org>). All online data were downloaded from Sept. 1, 2019 to Nov. 30, 2019.

3. Results

3.1. Plant components and paleoclimate

The plant assemblage consisted of 16 families, 23 genera, and 28 species in MK-1, while in MK-3, 27 families, 40 genera, and 54 species were identified (Table 1; Fig. 2; Plates S1, S2A, and S2B). The rarefaction analysis results indicate a higher plant diversity present in MK-3, regardless of the actual specimen numbers of entire fossil assemblages, or constrained sampling size numbers to the same level

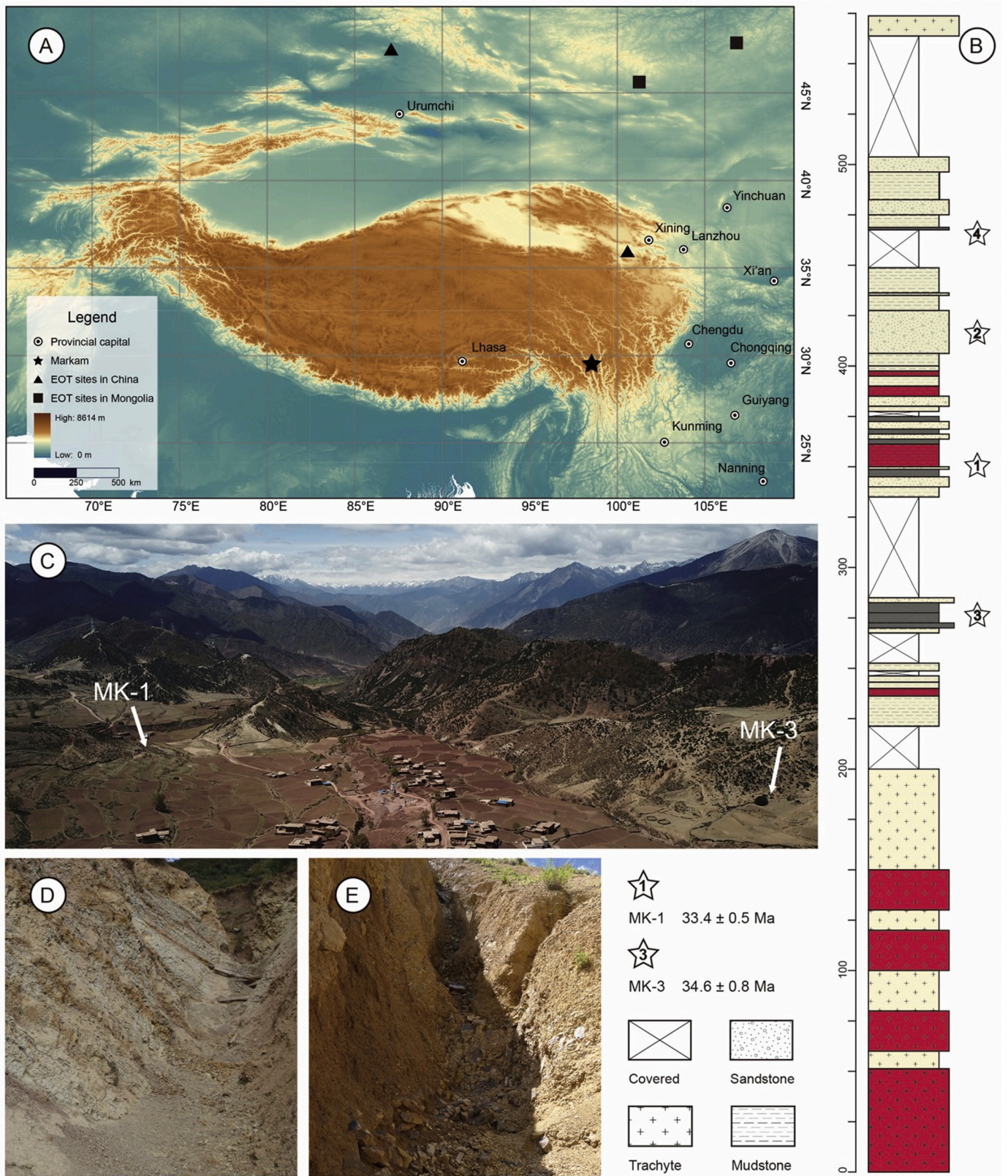


Fig. 1. (A) The Qinghai-Tibetan Plateau and the fossil localities which indicated the Eocene–Oligocene boundary in previous studies. The star marks the location of the Markam floras. The triangle represents the sections in the Xining Basin and the Junggar Basin in China. The rectangle represents sections in the Tsagaan Nur Basin and Taatsyn Gol in Mongolia. (B) Stratigraphic sections of the Lawula Formation and the fossiliferous layers in this study. Stars with numbers mark different plant-bearing layers. (C) Drone photo of the two fossil sites. (D) Fossil site of MK-1. (E) Fossil site of MK-3.

Table 1
Species list of MK-1 and MK-3 floristic assemblages, including all published and unpublished (with sp.) taxa.

Families	Species	Organs	MK-1	MK-3	
Equisetaceae	<i>Equisetum oppositum</i> Ma, Su et Zhang	Tuber	37	–	
Pinaceae	<i>Pinus</i> sp.	Leaf	5	35	
		Cone	–	9	
		Inflorescence	–	31	
		Seed	–	36	
	<i>Picea</i> sp.	Leaf	4	14	
	<i>Tsuga</i> sp.	Cone	–	4	
	<i>Abies</i> sp.	Cone	–	3	
Cupressaceae	<i>Chamaecyparis</i> sp.	Needle	–	18	
Lauraceae	<i>Lindera</i> sp.	Leaf	–	2	
Nelumbonaceae	<i>Nelumbo</i> sp. (cf. <i>N. nucifera</i>)?	Leaf	–	1	
(monocots)	(Monocotyledon)	Leaf	37	–	
Cercidiphyllaceae	<i>Cercidiphyllum</i> sp.?	Leaf	–	4	
Rosaceae	<i>Rubus</i> sp.	Leaf	–	1	
	<i>Rosa</i> sp.1	Leaf	27	–	
	<i>Rosa</i> sp.2	Leaf	–	4	
	<i>Rosa</i> sp.3	Leaf	–	18	
	<i>Cercocarpus</i> sp. (cf. <i>C. henricksonii</i>)	Leaf	19	–	
	<i>Cercocarpus</i> sp.2	Leaf	–	1	
	<i>Spiraea</i> sp. (cf. <i>S. betulifolia</i>)	Leaf	34	–	
	<i>Spiraea</i> sp.2	Leaf	88	–	
	<i>Pyracantha</i> sp.	Leaf	15	–	
	<i>Photinia</i> sp.	Leaf	–	2	
	<i>Cotoneaster</i> sp.1	Leaf	4	3	
	<i>Cotoneaster</i> sp.2	Leaf	11	–	
	<i>Cotoneaster</i> sp.3	Leaf	7	–	
	<i>Sorbus</i> sp.	Leaf	16	–	
	Elaeagnaceae	<i>Elaeagnus tibetensis</i> T. Su et Z. K. Zhou	Leaf	–	17
	Rhamnaceae	<i>Berhamniphyllum junrongiae</i> Z. K. Zhou, T. X. Wang et J. Huang	Leaf	–	2
	Urticaceae	<i>Oreocnide</i> sp.	Leaf	26	–
	Fagaceae	<i>Lithocarpus</i> sp.	Leaf	–	3
		<i>Castanopsis tibetensis</i> T. Su et Z. K. Zhou	Leaf	–	1
<i>Castanopsis</i> sp.1		Leaf	–	4	
<i>Castanopsis</i> sp.2		Leaf	–	1	
<i>Quercus tibetensis</i> H. Xu, T. Su et Z.K. Zhou		Leaf	–	1324	
<i>Quercus</i> sp.1		Leaf	1	9	
		Cone	–	1	
		Leaf	–	54	
		Leaf	–	2	
		Leaf	14	22	
Juglandaceae	<i>Juglans</i> sp.	Leaf	–	4	
Betulaceae	<i>Alnus</i> sp.1	Leaf	8	–	
	<i>Alnus</i> sp.2 (cf. <i>A. ferdinandicoburgii</i> C. K. Schneid.)	Leaf	–	35	
		Inflorescence	–	6	
	<i>Betula</i> sp.	Leaf	2	–	
	<i>Betula</i> sp. (cf. <i>B. alnoides</i>)	Leaf	–	484	
		Inflorescence	–	1	
	<i>Carpinus</i> sp.	Leaf	–	3	
Salicaceae	<i>Salix</i> sp. (cf. <i>S. cardiophylla</i>)	Leaf	109	–	
	<i>Salix</i> sp.1	–	–	4	
	<i>Salix</i> sp.2	–	–	10	
	<i>Salix</i> sp.3	–	–	3	
	<i>Salix</i> sp.4	Leaf	5	–	
		Inflorescence	1	–	
	<i>Populus</i> sp.	Leaf	–	65	
Anacardiaceae	<i>Cottinus</i> sp.	Leaf	–	1	
Sapindaceae	<i>Acer</i> sp. (cf. <i>A. subpictum</i>)	Leaf	–	12	
		Fruit	–	3	
	<i>Acer</i> sp. (cf. <i>A. paxii</i>)	Leaf	–	6	
	<i>Acer</i> sp.1	Leaf	–	26	
	<i>Acer</i> sp.2	Leaf	–	1	
	<i>Acer</i> sp.3	Fruit	1	3	

Table 1 (continued)

Families	Species	Organs	MK-1	MK-3
Theaceae	<i>Stewartia</i> sp.	Leaf	–	3
	<i>Camellia</i> sp.	Leaf	–	3
Ericaceae	<i>Rhododendron</i> sp.1	Leaf	–	6
	<i>Rhododendron</i> sp.2	–	–	17
Acanthaceae	<i>Avicennia</i> sp.?	Leaf	–	3
Aquifoliaceae	<i>Ilex</i> sp.	Leaf	–	1
Adoxaceae	<i>Viburnum</i> sp.	Leaf	–	1
(Others)	Morphotype MK-1-1	Leaf	17	–
	Morphotype MK-1-2	Leaf	2	–
	Morphotype MK-1-3	Leaf	3	–
	Morphotype MK-1-4	Leaf	1	–
	Morphotype MK-1-5	Leaf	3	–
	Morphotype MK-1-6	Leaf	1	–
	Morphotype MK-1-7	Leaf	2	–
	Morphotype MK-3-1	Leaf	–	6
Morphotype MK-3-2	Leaf	–	3	
Morphotype MK-3-3	Leaf	–	2	
Morphotype MK-3-4	Leaf	–	2	
Morphotype MK-3-5	Leaf	–	1	
Morphotype MK-3-6	Leaf	–	1	
Morphotype MK-3-7	Leaf	–	1	
Morphotype MK-3-8	Leaf	–	1	
(Others)	(Not identified)	Leaf	188	242
		(Other organs)	2	98
(Total)		(Specimens)	690	2684

(Figs. 3B, 4A).

Of the gymnosperms, species in the families Pinaceae and Cupressaceae were more abundant in MK-3 than in MK-1. Some genera, such as *Abies*, *Tsuga*, and *Chamaecyparis*, were only found in the MK-3 assemblage (Plates S1, S2A). The preserved plant reproductive organs in MK-3, including cones, inflorescences, and seeds, were diverse, but none of them were found in MK-1.

Statistical analyses on angiosperms show that the most dominant plant taxa in MK-3 were Fagaceae (52.98%, mainly evergreen elements such as *Lithocarpus*, *Quercus* subgenus *Cyclobalanopsis*) and Betulaceae (19.71%, mainly *Alnus* and *Betula*); *Rosa* and *Salix* only accounted for 0.82% and 0.63%, respectively. In MK-1, the dominant taxa were Rosaceae (32.03%, mainly *Rosa*) and Salicaceae (16.67%, mainly *Salix*), whereas *Quercus* and *Betula* accounted for 2.17% and 0.29%, respectively. Apart from these dominant families (or genera), some of the genera which were less abundant in MK-3, such as *Acer* and *Alnus*, were rare in MK-1 (Table 1). There was only one *Acer* fruit in MK-1 (Plate S1: q21), and no *Acer* leaves were found. Other genera, including *Lindera*, *Elaeagnus*, *Berhamniphyllum*, and *Populus*, were not found in MK-1 (Plates S2A and S2B: e07, i16, j17, o31), and there were only seven genera co-occurring in both MK-3 and MK-1. This result indicates a tremendous floristic change from MK-3 to MK-1, where the dominant taxa in one assemblage became less abundant in another assemblage (Fig. 2).

According to paleoclimate reconstructions from three different models, the mean annual temperature (MAT) was higher in MK-3, where the upper limit values were all above 15 °C. In contrast, the MAT below 15 °C was obtained from MK-1 by most of the reconstruction methods (Table 2). The current MAT of the Markam region is estimated to be about 4.4 °C (WorldClim, <http://www.worldclim.org>), which implies a much lower MAT than the reconstruction results for both MK-1 and MK-3. The precipitation results show that the decrease in mean annual precipitation (MAP), concurrently with the decrease in wettest month precipitation (MPWET) was encountered from MK-3 to MK-1 (Table 2).

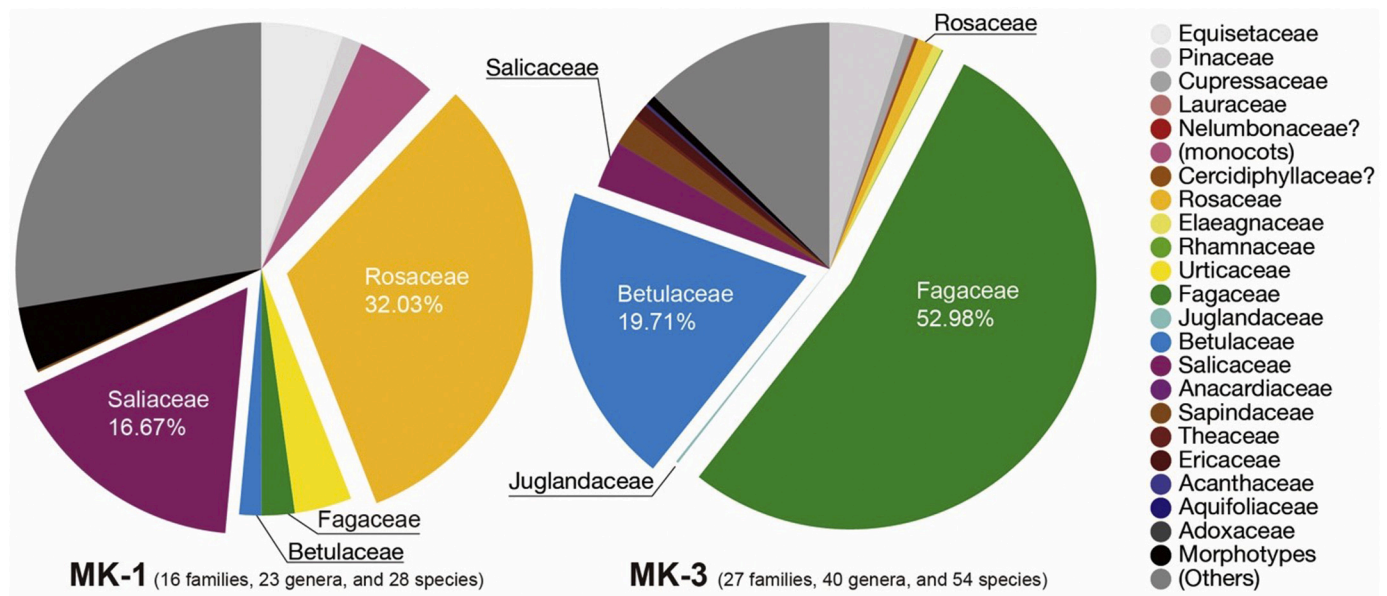


Fig. 2. Plant component comparison between MK-1 and MK-3. Different colors represent different families. The parts outstanding from the pie charts with percentages represent the dominant plant families in each assemblage.

3.2. Plant-herbivore interactions

A total of seven FFGs, namely hole feeding, margin feeding, skeletonization, surface feeding, piercing, mining, and galling (Fig. 5) were observed from the fossil leaf assemblages of MK-1 and MK-3. Due to the fundamental change of the floristic components from MK-3 to MK-1, the damage patterns of these two layers could not be comparable at genera or species levels. Regardless of this, the total damage frequency decreased from MK-3 (38.39%) to MK-1 (24.04%), and there are more individual leaves in MK-3 with more than two distinct DTs were present (Fig. 3A). Of the dominant families, Fagaceae and Betulaceae in MK-3 had a higher percentage of damaged leaves compared to Rosaceae and Salicaceae in MK-1.

Among the FFGs, hole feeding accounted for the largest functional feeding groups in both MK-1 and MK-3, followed by margin feeding (4.67%) and skeletonization (3.34%) in MK-1; whereas margin feeding (8.14%) and galling (4.16%) were relatively common FFGs in MK-3. Other FFGs that were commonly observed in MK-3 such as galling, were rare and only accounted for approximately 1% in MK-1. Apart from this, three FFGs including surface feeding, mining, and piercing, although not remarkable in MK-3, were not observed in MK-1 (Fig. 3A).

Based on standard rarefaction, the sample sizes were sufficient to represent herbivore damage of both MK-1 and MK-3 leaf assemblages. The result from the constrained analysis shows that in both generalized and specific FFGs, DTs were higher in MK-3 than in MK-1 (Figs. 3C, 4B–F), which might suggest higher herbivore diversity in MK-3 than in MK-1.

Table 2

Paleoclimatic variables estimated for the plant fossil assemblages MK-1 and MK-3. MAT1 (10° grid, CA); MAT2 (CLAMP, Su et al., 2019b); MAT3 (LMA); MTWM (mean temperature of the coldest month, CA); MTCM (mean temperature of the warmest month, CA); MAP (mean annual precipitation, CA); MPDRY (mean precipitation of the driest month, CA); MPWET (mean precipitation of the wettest month, CA).

	MAT1 (°C)	MAT2 (°C)	MAT3 (°C)	MTWM (°C)	MTCM (°C)	MAP (mm)	MPDRY (mm)	MPWET (mm)
MK-1	5.4–15.3	16.4 ± 2.3	10.4 ± 2.8	11.3–25.9	(–7.8)–7.8	357.8–1233.8	1–55.3	80.2–270.5
MK-3	7.2–17.6	17.8 ± 2.3	15.7 ± 2.4	14.2–29.5	(–3.4)–7.6	895.2–2195	10–55.3	145.2–435

4. Discussion

4.1. Plant diversity changes during the Eocene–Oligocene transition (EOT) on the southeastern Qinghai–Tibetan Plateau (QTP)

Paleoenvironmental changes during the EOT have contributed to a series of global biotic reorganization (Prothero, 1994; Xiao et al., 2010). Based on terrestrial faunal turnover, the extinction of Eurasian endemic mammals, such as the ‘Grande Coupure’ (Stehlin, 1909), was associated with climate deterioration by shifting to a drier climatic condition. Other biotic reorganizations involved molluscs (Hansen, 1987), otoliths (Ivany et al., 2000), and global vegetation (Pound and Salzmann, 2017). Changes in plant diversity during the EOT included the shift of evergreen forests to tundra in Antarctica (Thorn and DeConto, 2006), whereas the slow decline of plant diversity in Oregon implies the shifting of tropical floras to grassland at that time (Retallack, 2001). In China, multidisciplinary studies documented biotic turnover synchronously with climate change in the Junggar Basin (Northwestern China), where vegetation was changed from warm-temperate to dry-temperate climate forest with evidence from palynological investigation (Sun et al., 2014). Our study provides the first macrofossil evidence for plant diversity changes during the EOT in China.

Plant fossil assemblages from two layers in the Markam Basin suggest a sharp change in plant diversity during the EOT. Accordingly, the vegetation changed from a subtropical forest to alpine shrubland. The high species turnover is evidenced by the species richness: 27 families, dominated by Fagaceae and Betulaceae, in MK-3, compared to the 16 families of mainly Rosaceae and Salicaceae in MK-1 (Table 1). Moreover, there are mainly subtropical elements such as Lauraceae, Juglandaceae, and Elaeagnaceae in MK-3, and leaf sizes of most species in

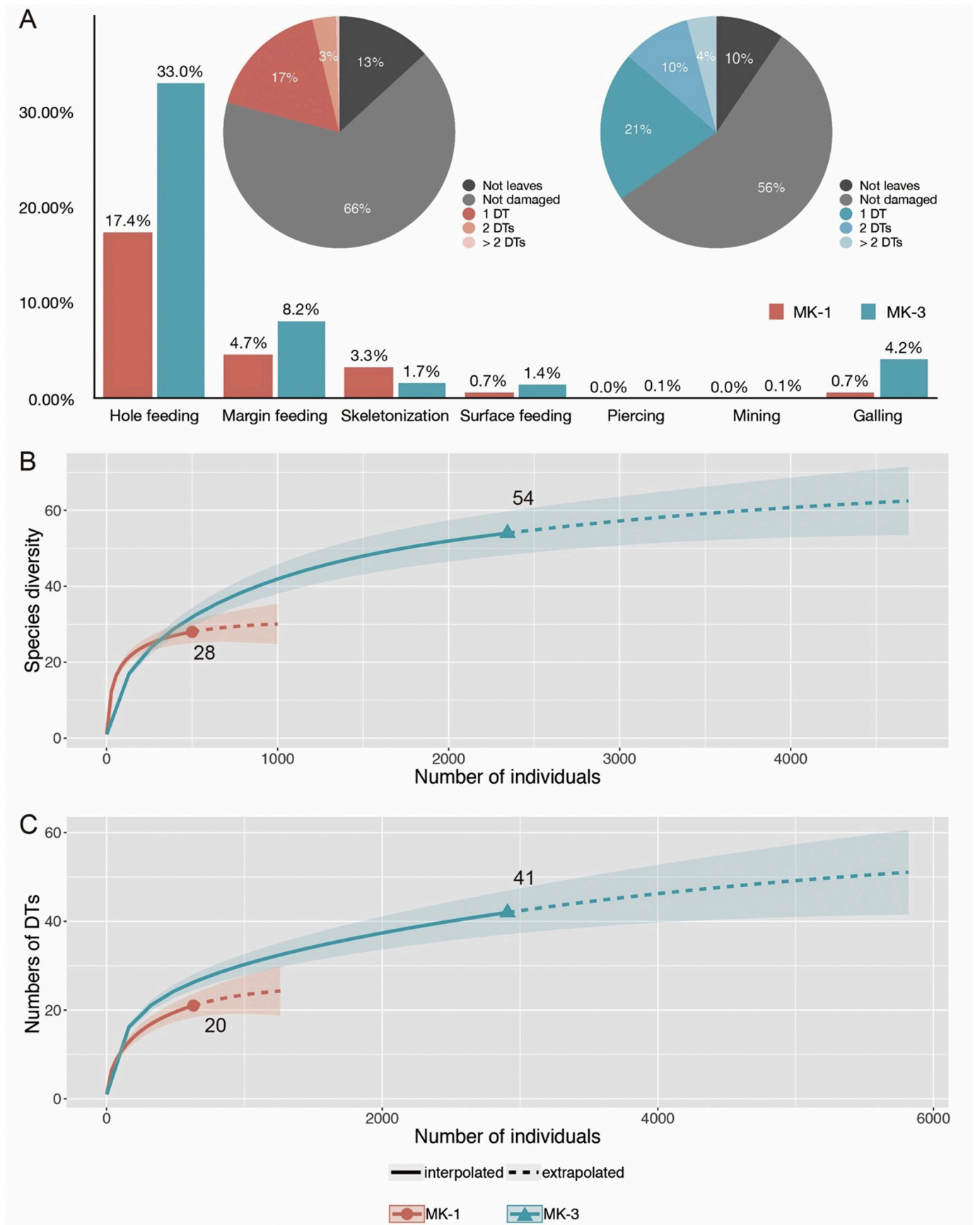


Fig. 3. (A) Histogram showing the percentages of different functional feeding groups occurs on fossil leaves; pie charts illustrate the percentages of leaves, other fossils, and the numbers of different damage types onto leaves. (B) Rarefaction curve of species diversity, including all the specimens sampled in the layer. (C) Rarefaction curve of damage type diversity, including all the specimens sampled in the layer.

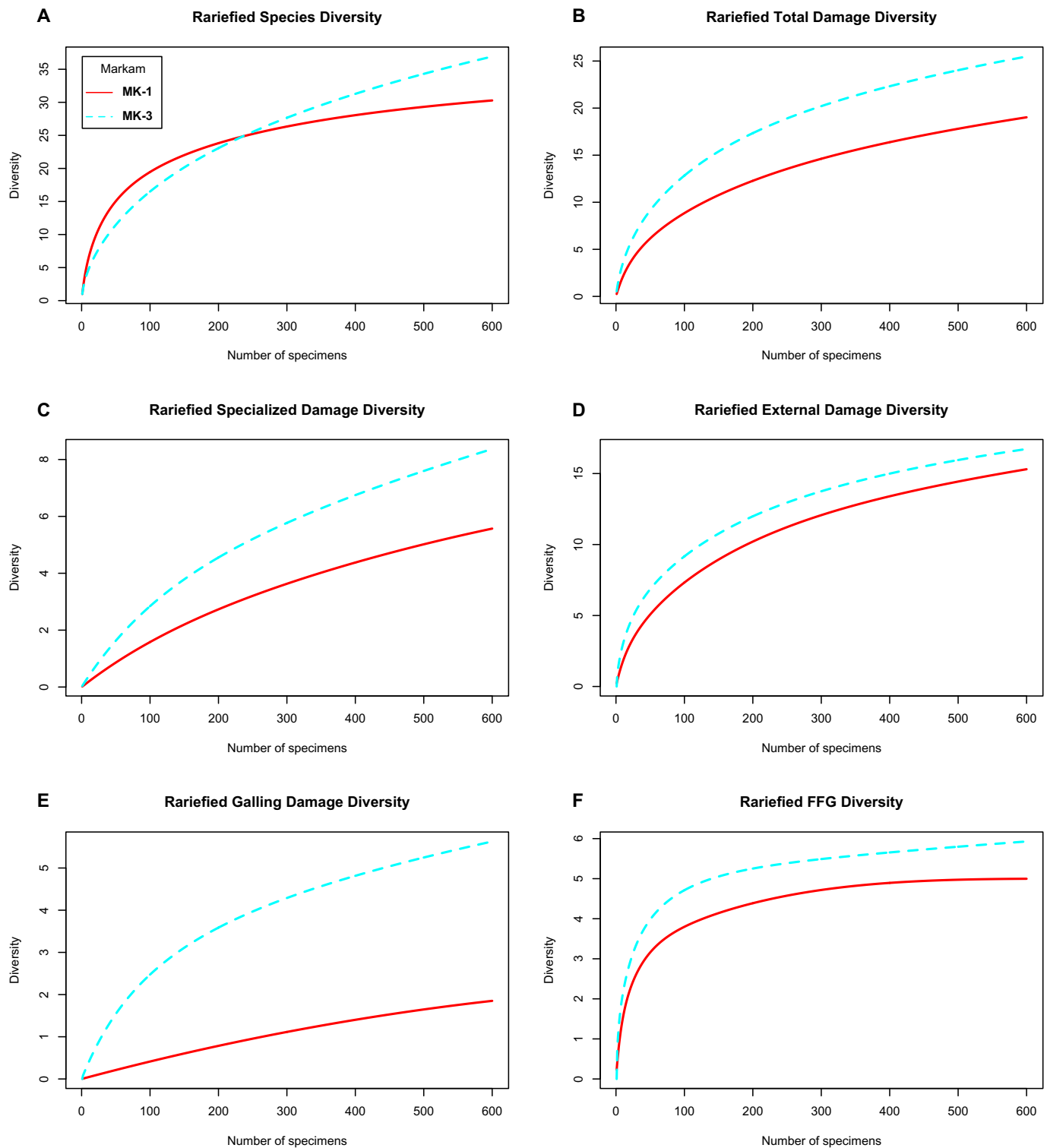


Fig. 4. Rarefaction curves of different index comparisons between MK-1 and MK-3, resampled to 600 leaves.

MK-3 were obviously larger than those in MK-1. The floristic components of the MK-1 assemblage mainly comprised Rosaceae, Salicaceae and other deciduous taxa with small leaves, indicating the presence of alpine shrubs.

Plant assemblage MK-3 is comparable to the fossil flora from the Jianchuan Basin in northwestern Yunnan, which is also dominated by Fagaceae (Tao, 2000). This megaflora was previously regarded as the Miocene in age (Tao, 2000). Recently, the plant-bearing Shuanghe Formation has been dated back to the late Eocene (~35 Ma) (Gourbet

et al., 2017). However, regarding the floristic assemblage of MK-1, it is not comparable to the early Oligocene Lühe flora (~32 Ma) from south-central Yunnan, which was dominated by Betulaceae (Linnemann et al., 2018). Therefore, the spatial differentiation of floristic components in southeastern margin of the QTP indicates that the EOT is an important period in shaping the regional division of plant diversity; this trend has also been observed in other places (Dupont-Nivet et al., 2008; Sun et al., 2014).

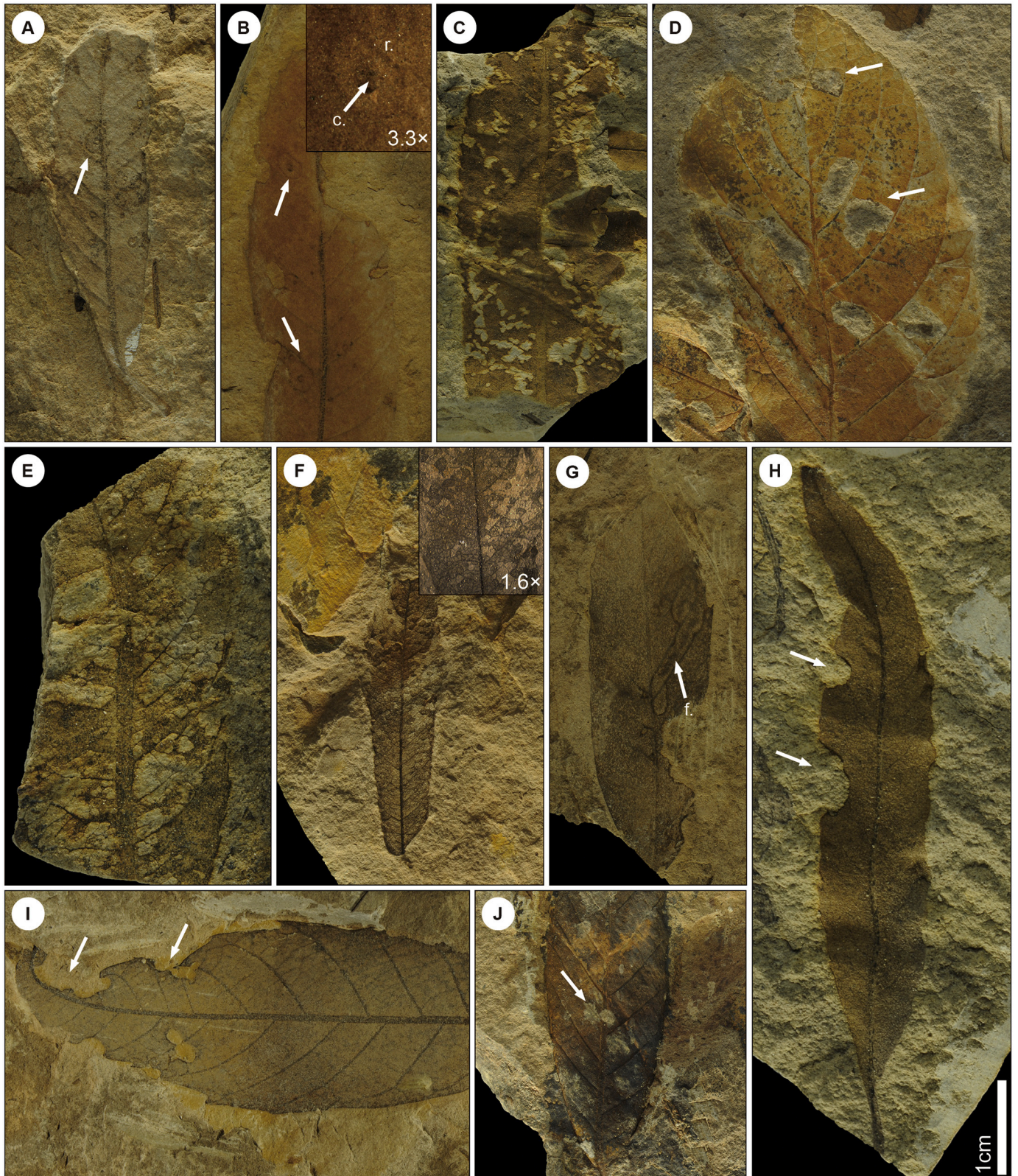


Fig. 5. Morphologies of some functional feeding groups. (A, B) Leaf galling from MK-3 (*Quercus tibetensis*). (A) shows a wide rim of thick tissue (DT11), and (B) with a core surrounded by outer rim (DT49, c. = core, r. = rim). (C) Hole feeding from MK-1 (*Rosa* sp.). (D) Hole feeding from MK-3 (*Alnus* sp.). (E, F) Skeletonization from MK-1 (*Salix* sp.) and MK-3 (*Salix* sp.), with or without the well-developed reaction rim (DT17, DT16). (G) 4725 Mining from MK-3 (*Q. tibetensis*), undefined, along the second vein with frass filled (f. = frass). (H, I) Margin feeding from MK-1 (*Spiraea* sp.) and MK-3 (*Q. tibetensis*), less than 180 degrees of arc (DT12). (J) Non-herbivore physical damages.

4.2. Paleoclimate change during the EOT on the southeastern QTP

Currently, our understanding of the paleoenvironmental conditions on the QTP is still far from being sufficient, because different parts of the QTP experienced asynchronous uplift (Su et al., 2019a; Valdes et al., 2019). The Markam Basin, located at southeastern marginal part of the QTP, experienced dramatic paleoclimatic changes during the EOT. According to this study, using LMA, the MAT in MK-3 and MK-1 were 15.7 °C and 10.4 °C, respectively, which is further supported by results based on the CA (Table 2). Therefore, the climatic condition during the late Eocene must have been largely different from that presently occurring in the southeastern margin of the QTP. This is in agreement with a recent study from the Jianchuan Basin (Gourbet et al., 2017). Specifically, Sorrel et al. (2017) suggested a wet and even tropical climate during ~35.5 Ma in the Jianchuan Basin via sedimentological data. Both pieces of evidence are consistent with the global climate condition at that time (Zachos et al., 2001). However, the climatic conditions of different parts on the plateau were not the same, and a palynological study from the Xining Basin in northern QTP proved an aridification trend during the late Eocene (Licht et al., 2014).

Via CA, the early Oligocene floristic assemblage MK-1 indicates a sharp temperature decline, with a MAT 1.8–2.3 °C lower than that of the MK-3. This might be due to both global cooling as well as the uplift of southeastern margin of the QTP, because the global climate change could not fully explain such dramatic temperature decline, the early Oligocene Lühe flora showed a much warmer climate than that in Markam at the same time (Linnemann et al., 2018). On the other hand, the latest paleobotanical evidence with calibrated ⁴⁰Ar/³⁹Ar ages suggests that the mountain in the Markam Basin was uplifted from ~2800 m (MK-3) to ~3800 m (MK-1) within ~1 million years, almost reaching its present elevation (Su et al., 2019b). It should be mentioned that the climate change during the EOT could not be only represented by the changes in temperature, but also by a decrease in precipitation (Table 2). More paleoclimatic studies with different proxies are needed in future to better understand the paleoclimate history in this region.

4.3. Plant-herbivore interactions in response to paleoenvironmental changes

Increasing paleontological evidence on the QTP has improved our understanding of the plateau formation as well as the evolutionary history of biodiversity in this large region (Dupont-Nivet et al., 2008; Deng et al., 2011; Wu et al., 2017; Su et al., 2019b; Deng et al., 2020). As mentioned above, the significant changes in floristic assemblages occurred simultaneously with the sharp decrease in temperature during the EOT in southeastern margin of the QTP. However, as the most important biotic relationships in terrestrial ecosystems, reports of fossil plant-herbivore interactions are limited in this region. Therefore, this study provides solid evidence that paleoenvironmental changes shaped plant-herbivore interactions during the EOT on the plateau.

Concurrent with the sharp replacement of host plants, the obligate parasites were faced with huge pressures. Galling and mining decreased or even disappeared as a result of changed host types (Fig. 3). The total DF and DTs changes are remarkable. Overall, 21 DTs, representing different values of host specificity, were lost from MK-3 to MK-1. This reflects the diversity decrease of both general and specific herbivores. The approximately 15% decrease in DF indicates lower herbivore quantities and leaf consumption after the EOT. Most of the DTs are mainly determined by the mouthpart and the behavior of herbivores (Labandeira, 1997, 2019; Chapman and Chapman, 1998). Of the fossil leaves in MK-3, specific mining indicates consumers of likely Lepidoptera miners, which are commonly documented on extant Fagaceae leaves (Bultman and Faeth, 1986; Boecklen and Spellenberg, 1990). Because number of damage types is good indicator of herbivore diversity (Carvalho et al., 2014), the shrinkage or absent of these DTs in MK-1, might imply the diminution or extinction of some typical host herbivores from this region.

Changes in plant-herbivore interactions likely correlate with the regional climate changes, where temperature fluctuations contribute to changes in herbivore DF and DTs. In concordance to the temperature drops in the Markam Basin, the DF and DTs from the middle elevational (~2800 m) subtropical region of MK-3 showed higher index values than those obtained from the high-elevation (~3800 m) shrubland region of MK-1. This indicates that temperature change is vital in manipulating plant-herbivore interactions, where the higher diversity of DTs and DF is driven by the temperature rise. A similar finding was obtained from modern sampling studies revealing that the DF and DTs increased from subtropical to tropical regions (Adams et al., 2010; Roslin et al., 2017). The same behavior trend of insect herbivory has been reported for the Paleocene–Eocene Thermal Maximum (PETM, 55.8 Ma) (Currano et al., 2008; Wappler et al., 2012; Pinheiro et al., 2016). Synchronous DF and DTs changes have been observed accompanying by climatic changes before the Oligocene–Miocene transition (OMT) in Germany (Wappler, 2010). Compared to these fossil sites, the damage diversity in each plant family from both MK-1 and MK-3 is lower probably due to the herbivory and plant evolution. However, the proportion of damaged leaves in the two assemblages is higher than the OMT sites, which is congruent with the higher temperature in the EOT (Zachos et al., 2001).

Regardless of the specific precipitation-sensitive herbivores and plants groups, the changes in vegetation types and leaf sizes are evidence for a precipitation decrease from MK-3 to MK-1 (Wright et al., 2017). Some herbivory interactions such as galling, can also be used to trace changes in humidity (Fernandes and Price, 1992; Adroit et al., 2016). However, these methods to trace humidity changes require DF and DTs comparison within same plant species, and their corresponding herbivores are impossible to apply in the Markam flora due to fundamental changes in the entire fossil flora. The pattern in this study is also significantly different from the relatively stable plant-herbivore interactions in evergreen sclerophyllous oak forests of southeastern margin of the QTP during Quaternary climate fluctuations (Su et al., 2015).

In general, the EOT is an important period for the turnover of biota on the QTP. The global dramatic climate changes in conjunction with the QTP uplift led to a significant change in plant diversity and plant-herbivore interactions, and progressively shaped the unique biodiversity as well as the entire ecosystem in this region.

Declaration of Competing Interest

None.

Acknowledgments

We thank members of Paleoecology Research Group (PRG) in Xishuangbanna Tropical Botanical Garden (XTBG) for fossil collecting on the Qinghai-Tibetan Plateau; Dr. Gaurav Srivastava from Birbal Sahni Institution, Dr. Yu Song from Xishuangbanna Tropical Botanical Garden (XTBG) for their help on leaf fossil identification; the Public Technology Service Center, XTBG for help with imaging. This work is supported by the National Natural Science Foundation of China (Nos. 41661134049, 41922010); Second Tibetan Plateau Scientific Expedition and Research Grant (No. 2019QZKK0705); the Strategic Priority Research Program, CAS (Nos. XDA 20070301, XDB 26000000); the Key Research Program of Frontier Sciences, CAS (No. QYZDB-SSW-SMC016); Youth Innovation Promotion Association, CAS (No. 2017439); and the CAS 135 program (No. 2017XTBG-F01).

Appendix A. Supplementary data

Supplementary data to this article can be found online at <https://doi.org/10.1016/j.gloplacha.2020.103293>.

References

- Abels, H.A., Dupont-Nivet, G., Xiao, G., Bosboom, R., Krijgsman, W., 2011. Step-wise change of Asian interior climate preceding the Eocene–Oligocene transition (EOT). *Palaeogeogr. Palaeoclimatol. Palaeoecol.* 299, 399–412.
- Adams, J.M., Brusa, A., Soyeong, A., Ainuddin, A., 2010. Present-day testing of a paleoecological pattern: is there really a latitudinal difference in leaf-feeding insect-damage diversity? *Rev. Palaeobot. Palynol.* 162 (1), 63–70.
- Adams, J.M., Ahn, S., Ainuddin, N., Lee, M.-L., 2011. A further test of a paleoecological thermometer: tropical rainforests have more herbivore damage diversity than temperate forests. *Rev. Palaeobot. Palynol.* 164 (1–2), 60–66.
- Adroit, B., Wappler, T., Terral, J.-F., Ali, A.A., Girard, V., 2016. Bernasso, a paleoforest from the early Pleistocene: New input from plant-insect interactions (Hérault, France). *Palaeogeogr. Palaeoclimatol. Palaeoecol.* 446, 78–84.
- Adroit, B., Malekhosseini, M., Girard, V., Abedi, M., Rajaei, H., Terral, J.-F., Wappler, T., 2018. Changes in pattern of plant-insect interactions on the Persian ironwood (*Parrotia persica*, Hamamelidaceae) over the last 3 million years. *Rev. Palaeobot. Palynol.* 258, 22–35.
- Allen, M.B., Armstrong, H.A., 2008. Arabia–Eurasia collision and the forcing of mid-Cenozoic global cooling. *Palaeogeogr. Palaeoclimatol. Palaeoecol.* 265 (1), 52–58.
- Bale, J.S., Masters, G.J., Hodkinson, I.D., Awmack, C.S., Bezemer, T.M., Brown, V.K., Butterfield, J., Buse, A., Coulson, J.C., Farrar, J., 2002. Herbivory in global climate change research: direct effects of rising temperature on insect herbivores. *Glob. Chang. Biol.* 8 (1), 1–16.
- Basak, C., Martin, E.E., 2013. Antarctic weathering and carbonate compensation at the Eocene–Oligocene transition. *Nat. Geosci.* 6 (2), 121–124.
- Berry, E.W., 1916. *The lower Eocene floras of southeastern North America*, 91. US Government Printing Office.
- Blois, J.L., Zarnetske, P.L., Fitzpatrick, M.C., Finnegan, S., 2013. Climate change and the past, present, and future of biotic interactions. *Science* 341 (6145), 499–504.
- Boecklen, W.J., Spellenberg, R., 1990. Structure of herbivore communities in two oak (*Quercus* spp.) hybrid zones. *Oecologia* 85 (1), 92–100.
- Bultman, T.L., Faeth, S.H., 1986. Leaf size selection by leaf-mining insects on *Quercus emoryi* (Fagaceae). *Oikos* 46, 311–316.
- Carvalho, M.R., Wilf, P., Barrios, H., Windsor, D.M., Currano, E.D., Labandeira, C.C., Jaramillo, C.A., 2014. Insect leaf-chewing damage tracks herbivore richness in modern and ancient forests. *PLoS One* 9 (5), e94950.
- Chao, A., Gotelli, N.J., Hsieh, T.C., Sander, E.L., Ma, K.H., Colwell, R.K., Ellison, A.M., 2014. Rarefaction and extrapolation with Hill numbers: a framework for sampling and estimation in species diversity studies. *Ecol. Monogr.* 84 (1), 45–67.
- Chapman, R.F., Chapman, R.F., 1998. *The Insects: Structure and Function*. Cambridge University Press.
- Colwell, R.K., Anne, C., Nicholas, J.G., Lin, S.Y., Chang, X.M., Robin, L.C., John, T.L., 2012. Models and estimators linking individual-based and sample-based rarefaction, extrapolation and comparison of assemblages. *J. Plant Ecol.* 5 (1), 3–21.
- Currano, E.D., Wilf, P., Wing, S.L., Labandiera, C.C., Lovelock, E.C., Royer, D.L., 2008. Sharply increased insect herbivory during the Paleocene–Eocene thermal Maximum. *Proc. Natl. Acad. Sci. U. S. A.* 105 (6), 1960–1964.
- Deng, T., Wang, X.M., Fortelius, M., Li, Q., Wang, Y., Tseng, Z.J., Takeuchi, G.T., Saylor, J.E., Salla, L.K., Xie, G.P., 2011. Out of Tibet: Pliocene woolly rhino suggests high-plateau origin of Ice Age megaherbivores. *Science* 333 (6047), 1285–1288.
- Deng, T., Wu, F., Zhou, Z., Su, T., 2020. Tibetan Plateau: an evolutionary junction for the history of modern biodiversity. *Sci. China-Earth Sci.* 63, 172–187.
- Dupont-Nivet, G., Hoorn, C., Konert, M., 2008. Tibetan uplift prior to the Eocene–Oligocene climate transition: evidence from pollen analysis of the Xining Basin. *Geology* 37 (6), 987–990.
- Fernandes, G.W., Price, P.W., 1992. The adaptive significance of insect gall distribution: survivorship of species in xeric and Mesic habitats. *Oecologia* 90 (1), 14–20.
- Gourbet, L., Leloup, P.H., Paquette, J.-L., Sorrel, P., Maheo, G., Wang, G., Xu, Y., Cao, K., Antoine, P.O., Eymard, I., Liu, W., Lu, H., Replumaz, A., Chevalier, M.-L., Zhang, K., Jing, W., Shen, T., 2017. Reappraisal of the Jianchuan Cenozoic basin stratigraphy and its implications on the SE Tibetan Plateau evolution. *Tectonophysics* 700, 162–179.
- Gunkel, S., Wappler, T., 2015. Plant-insect interactions in the upper Oligocene of Enspel (Westerwald, Germany), including an extended mathematical framework for rarefaction. *Palaeobio. Palaeoenv.* 95 (1), 55–75.
- Hansen, T.A., 1987. Extinction of late Eocene to Oligocene molluscs: Relationship to shelf area, temperature changes, and impact events. *Palaios* 2, 69–75.
- Hooker, J.J., Collinson, M.E., Sille, N.P., 2004. Eocene–Oligocene mammalian faunal turnover in the Hampshire Basin, UK: calibration to the global time scale and the major cooling event. *J. Geol. Soc.* 161 (2), 161–172.
- Ivany, L.C., Patterson, W.P., Lohmann, K.C., 2000. Cooler winter as a possible cause of mass extinctions at the Eocene/Oligocene boundary. *Nature* 407, 887–890.
- Katz, M.E., Miller, K.G., Wright, J.D., Wade, B.S., Browning, J.V., Cramer, B.S., Rosenthal, Y., 2008. Stepwise transition from the Eocene greenhouse to the Oligocene icehouse. *Nat. Geosci.* 1 (5), 329–334.
- Labandeira, C.C., 1997. Insect mouthparts: ascertaining the paleobiology of insect feeding strategies. *Annu. Rev. Ecol. Syst.* 28 (1), 153–193.
- Labandeira, C.C., 2019. The fossil record of insect mouthparts: innovation, functional convergence, and associations with other organisms. In: Krenn, H.W. (Ed.), *Insect Mouthparts: Form, Function, Development and Performance*. Springer International Publishing, pp. 567–671.
- Labandeira, C.C., Wilf, P., Johnson, K.R., Marsh, F., 2007. *Guide to Insect (and Other) Damage Types on Compressed Plant Fossils*. Smithsonian Institution, National Museum of Natural History, Department of Paleobiology, Washington, DC.
- Licht, A., Van Cappelle, M., Abels, H.A., Ladant, J., Trabuco-Alexandre, J., France-lanord, C., Donnadiou, Y., Vandenberghe, J., Rigaudier, T., Lecuyer, C., Terry Jr., D., Adriaens, R., Boura, A., Guo, Z., 2014. Aung Naing Soe, Quade, J., Dupont-Nivet, G., Jaeger J.-J., 2014. Asian monsoons in a late Eocene greenhouse world. *Nature* 513, 501–506.
- Linnemann, U., Su, T., Kunzmann, L., Spicer, R.A., Ding, W., Spicer, T.R.V., Zieger, J., Hofmann, M., Morawek, K., Gärtner, A., Gerdes, A., Marko, L., Zhang, S., Li, S., Tang, H., Huang, J., Mulch, A., Mosbrugger, V., Zhou, Z., 2018. New U–Pb dates show a Palaeogene origin for the modern Asian biodiversity hot spots. *Geology* 46 (1), 3–6.
- Liu, Z., Pagani, M., Zinniker, D., DeConto, R., Huber, M., Brinkhuis, H., Shah, S.R., Leckie, R.M., Pearson, A., 2009. Global cooling during the Eocene–Oligocene climate transition. *Science* 323 (5918), 1187–1190.
- Loughnan, D., Williams, J.L., 2018. Climate and leaf traits, not latitude, explain variation in plant-herbivore interactions across a species' range. *J. Ecol.* 107 (2), 913–922.
- Ma, H., Zhang, S., Su, T., Sui, S., 2012. New materials of *Equisetum* from the Upper Miocene of Mangkang, eastern Xizang and its ecological implications. *J. Jilin Univ. (Earth Sci. Ed.)* 42 (s3), 189–195.
- Manchester, S.R., 2001. Update on the megafossil flora of Florissant, Colorado, Fossil flora and stratigraphy of the Florissant Formation, Colorado. *Proceedings of the Denver Museum of Nature and Science* 137–162.
- Massad, T.J., Dyer, L.A., 2010. A meta-analysis of the effects of global environmental change on plant-herbivore interactions. *Arthropod-Plant Int.* 4 (3), 181–188.
- Meng, J., McKenna, M.C., 1998. Faunal turnovers of Palaeogene mammals from the Mongolian Plateau. *Nature* 394 (6691), 364.
- Mosbrugger, V., Utescher, T., 1997. The coexistence approach—a method for quantitative reconstructions of Tertiary terrestrial palaeoclimate data using plant fossils. *Palaeogeogr. Palaeoclimatol. Palaeoecol.* 134 (1–4), 61–86.
- Paik, I.S., Kim, G.J., Kim, K., Jeong, E.K., Kang, H.C., Lee, H.I., Uemura, K., 2012. Leaf beds in the early Miocene lacustrine deposits of the Geumgwangdong Formation, Korea: Occurrence, plant-insect interaction records, taphonomy and palaeoenvironmental implications. *Rev. Palaeobot. Palynol.* 170 (1–14), 1–14.
- Pinheiro, E.R., Iannuzzi, R., Duarte, L.D., 2016. Insect herbivory fluctuations through geological time. *Ecology* 97 (9), 2501–2510.
- Pound, M.J., Salzmann, U., 2017. Heterogeneity in global vegetation and terrestrial climate change during the late Eocene to early Oligocene transition. *Sci. Rep.* 7, 43386.
- Price, P.W., 2002. Resource-driven terrestrial interaction webs. *Ecol. Res.* 17 (2), 241–247.
- Prothero, D.R., 1994. The late Eocene–Oligocene extinctions. *Annu. Rev. Earth Pl. Sc.* 22, 145–165.
- Retallack, G.J., 2001. Cenozoic expansion of Grasslands and Climatic Cooling. *J. Geol.* 109 (4), 407–426.
- Roslin, T., Hardwick, B., Novotny, V., Petry, W.K., Andrew, N.R., Asmus, A., Barrio, I.C., Basset, Y., Boesing, A.L., Bonebrake, T.C., Cameron, E.K., Dáttilo, W., Donoso, D.A., Drozd, P., Gray, C.L., Hik, D.S., Hill, S.J., Hopkins, T., Huang, S., Koane, B., Laird-Hopkins, B., Laukkanen, L., Lewis, O.T., Milne, S., Mwesige, I., Nakamura, A., Nell, C.S., Nichols, Elizabeth, Prokurat, A., Sam, K., Schmidt, N.M., Slade, A., Slade, V., Suchanková, A., Teder, T., Nouhuys, S., Vandvik, V., Weissflog, A., Zhukovich, V., Slade, E.M., 2017. Higher predation risk for insect prey at low latitudes and elevations. *Science* 356 (6339), 742–744.
- Sam, K., Koane, B., Sam, L., Mrazova, A., Segar, S., Volf, M., Moos, M., Simek, P., Sisol, M., Novotny, V., 2020. Insect herbivory and herbivores of *Ficus* species along a rain forest elevational gradient in Papua New Guinea. *Biotropica* 52 (2), 263–276.
- Schachat, S.R., Labandeira, C.C., Maccracken, S.A., 2018. The importance of sampling standardization for comparisons of insect herbivory in deep time: a case study from the late Palaeozoic. *R. Soc. Open Sci.* 5, 171991.
- Schachat, S.R., Maccracken, S.A., Labandeira, C.C., 2020. Sampling fossil floras for the study of insect herbivory: how many leaves is enough? *Foss. Rec.* 23, 15–32.
- Schoonhoven, L.M., Van Loon, J.J., Dicke, M., 2005. *Insect–Plant Biology*, second ed. Oxford University, New York.
- Sohn, J.C., Kim, N.H., Choi, S.W., 2019. Effect of elevation on the insect herbivory of Mongolian oaks in the high mountains of southern South Korea. *J. Asia Pac. Entomol.* 22, 957–962.
- Sorrel, P., Eymard, I., Leloup, P.H., Maheo, G., Olivier, N., Sterb, M., Gourbet, L., Wang, G., Jing, W., Lu, H., Li, H., Yadong, X., Zhang, K., Cao, K., Chevalier, M.-L., Replumaz, A., 2017. Wet tropical climate in SE Tibet during the late Eocene. *Sci. Rep.* 7, 7809.
- Stehlin, H.G., 1909. Remarques sur les faunes de mammifères des couches éocènes et oligocènes du Bassin de Paris. *Bull. Soc. Géol. France* 19, 488–520.
- Su, T., Xing, Y., Liu, Y., Jacques, F.M.B., Chen, W., Huang, Y., Zhou, Z., 2010. Leaf margin analysis: a new equation from humid to Mesic forests in China. *Palaios* 25 (4), 234–238.
- Su, T., Wilf, P., Xu, H., Zhou, Z., 2014. Miocene leaves of *Elaeagnus* (Elaeagnaceae) from the Qinghai-Tibet Plateau, its modern center of diversity and endemism. *Am. J. Bot.* 101 (8), 1350–1361.
- Su, T., Adams, J.M., Wappler, T., Huang, Y.J., Jacques, F.M.B., Liu, Y.S., Zhou, Z., 2015. Resilience of plant–insect interactions in an oak lineage through Quaternary climate change. *Paleobiology* 41 (1), 174–186.
- Su, T., Farnsworth, A., Spicer, R.A., Huang, J., Wu, F., Liu, J., Li, S., Xing, Y., Huang, Y., Deng, W., Tang, H., Xu, C., Zhao, F., Guarav, S., Paul, J.V., Deng, T., Zhou, Z., 2019a. No high Tibetan Plateau until the Neogene. *Sci. Adv.* 5 (3), 2189.
- Su, T., Spicer, R.A., Li, S., Xu, H., Huang, J., Sarah, A., Huang, Y., Li, S., Wang, L., Jia, L., Deng, D., Liu, J., Deng, C., Zhang, S., Paul, J.V., Zhou, Z., 2019b. Uplift, climate and biotic changes at the Eocene–Oligocene transition in South-Eastern Tibet. *Nat. Sci. Rev.* 6 (3), 495–504.
- Sun, J., Ni, X., Bi, S., Wu, W., Ye, J., Meng, J., Windley, B., 2014. Synchronous turnover of flora, fauna, and climate at the Eocene–Oligocene Boundary in Asia. *Sci. Rep.* 4, 7463.

- Tao, J., 2000. The Evolution of the Late Cretaceous–Cenozoic Flora in China. Science Press, Beijing.
- Thorn, V.C., DeConto, R., 2006. Antarctica climate at the Eocene/Oligocene boundary—climate model sensitivity to high latitude vegetation type and comparisons with the palaeobotanical record. *Palaeogeogr. Palaeoclimatol. Palaeoecol.* 231, 134–157.
- Tylianakis, J.M., Didham, R.K., Bascompte, J., Wardle, D.A., 2008. Global change and species interactions in terrestrial ecosystems. *Ecol. Lett.* 11 (12), 1351–1363.
- Valdes, P.J., Ding, L., Farnsworth, A., Spicer, R.A., Li, S., Li, S., Su, T., 2019. Comment on “revised paleoaltimetry data show low Tibetan Plateau elevation during the Eocene”. *Science* 365 (6459), 8474.
- Wappler, T., 2010. Insect herbivory close to the Oligocene–Miocene transition—a quantitative analysis. *Palaeogeogr. Palaeoclimatol. Palaeoecol.* 292, 540–550.
- Wappler, T., Currano, E.D., Wilf, P., Rust, J., Labandeira, C.C., 2009. No post-cretaceous ecosystem depression in European forests? Rich insect-feeding damage on diverse middle Palaeocene plants, Menat, France. *Proc. R. Soc. B-Biol. Sci.* 276 (1677), 4271–4277.
- Wappler, T., Labandeira, C.C., Rust, J., Frankenhäuser, H., Wilde, V., 2012. Testing for the effects and consequences of mid Paleogene climate change on insect herbivory. *PLoS One* 7, e40744.
- Wilf, P., Labandeira, C.C., 1999. Response of plant-insect associations to Paleocene–Eocene warming. *Science* 284, 2153–2156.
- Wright, I.J., Ning, D., Vincent, M., Prentice, I.C., Westoby, M., Sandra, D., Rachael, G., Bonnie, J., Robert, K., Law, E.A., Leishman, M.R., Niinements, Ü., Reich, P.B., Sack, L., Villar, R., Wang, H., Wilf, P., 2017. Global climatic drivers of leaf size. *Science* 357 (6354), 917–921.
- Wu, F., Miao, D., Chang, M., Shi, G., Wang, N., 2017. Fossil climbing perch and associated plant megafossils indicate a warm and wet Central Tibet during the late Oligocene. *Sci. Rep.* 7 (1), 878.
- Wu, M., Huang, J., Su, T., Leng, Q., Zhou, Z., 2019. *Tsuga* seed cones from the late Paleogene of southwestern China and their biogeographical and paleoenvironmental implications. *Palaeoworld* (In press).
- Xiao, G., Abels, H., Yao, Q., Dupont-Nivet, G., Hilgen, F.J., 2010. Asian aridification linked to the first step of the Eocene–Oligocene climate transition (EOT) in obliquity-dominated terrestrial records (Xining Basin, China). *Clim. Past* 6, 627–657.
- Xu, H., Zhang, S., Deng, M., 2016. The first fossil record of ring-cupped oak (*Quercus* L. subgenus *Cyclobalanopsis* (Oersted) Schneider) in Tibet and its paleoenvironmental implications. *Palaeogeogr. Palaeoclimatol. Palaeoecol.* 442, 61–71.
- Xu, H., Su, T., Zhou, Z., 2019. Leaf and infructescence fossils of *Alnus* (Betulaceae) from the late Eocene of the southeastern Qinghai–Tibetan Plateau. *J. Syst. Evol.* 57 (2), 105–113.
- Zachos, J.C., Pagani, M., Sloan, L.C., Thomas, E., Billups, K., 2001. Trends, rhythms, and aberrations in global climate 65 Ma to present. *Science* 292 (5517), 686–693.
- Zhou, Z., Wang, T., Huang, J., Liu, J., Deng, W., Li, S., Deng, C., Su, T., 2020. Fossil leaves of *Berhamniphyllum* (Rhamnaceae) from Markam, Tibet and their biogeographic implications. *Sci. China-Earth Sci.* 63, 224–234.
- Zvereva, E., Kozlov, M., 2006. Consequences of simultaneous elevation of carbon dioxide and temperature for plant-herbivore interactions: a metaanalysis. *Glob. Chang. Biol.* 12 (1), 27–41.